Technical Note: Effect of Weld Pool Configuration on Heat-Affected Zone Shape

BY S. S. GLICKSTEIN AND E. FRIEDMAN

ABSTRACT. Irregular weld bead configurations resulting from the gas tungsten arc welding process have been observed and reported in the past for many different welding conditions. Although it would be expected that the outer boundary of the heat-affected zone would also have an irregular shape if that boundary were in close proximity to the weld metal, it has been observed that for stationary arc welds with alloy 600 material that the heat-affected zone consistently has a regular ellipsoidal shape.

A finite element heat conduction model was employed to demonstrate that the mechanism of conduction heat transfer is sufficient to completely damp out the effect of the weld bead irregularity on the shape of the isotherm representing the boundary of the heat-affected zone. An anomaly that has existed for some time has, therefore, been rationalized with the aid of computer modeling of the welding process.

Introduction

In the course of performing stationary gas tungsten arc welds on Inconel alloy 600 plates,[1,2] irregularly shaped weld bead heat-affected zone interfaces were observed from photomicrographs of weld cross sections. Typical weld bead and heat-affected zone configurations are presented in Fig. 1. The irregularly shaped interface was unexpected and paradoxical. The shape of the interface is in conflict with results obtained from a heat conduction analysis used to calculate isotherms in the weldments and to predict the shape of the molten weld pool during stationary gas tungsten arc welding.[1]

In the first reference,[1] it was conjectured that weld pool motion (in particular the circulation of two weld puddles[3,4]) during the stationary arc welding of alloy 600 may be the cause of

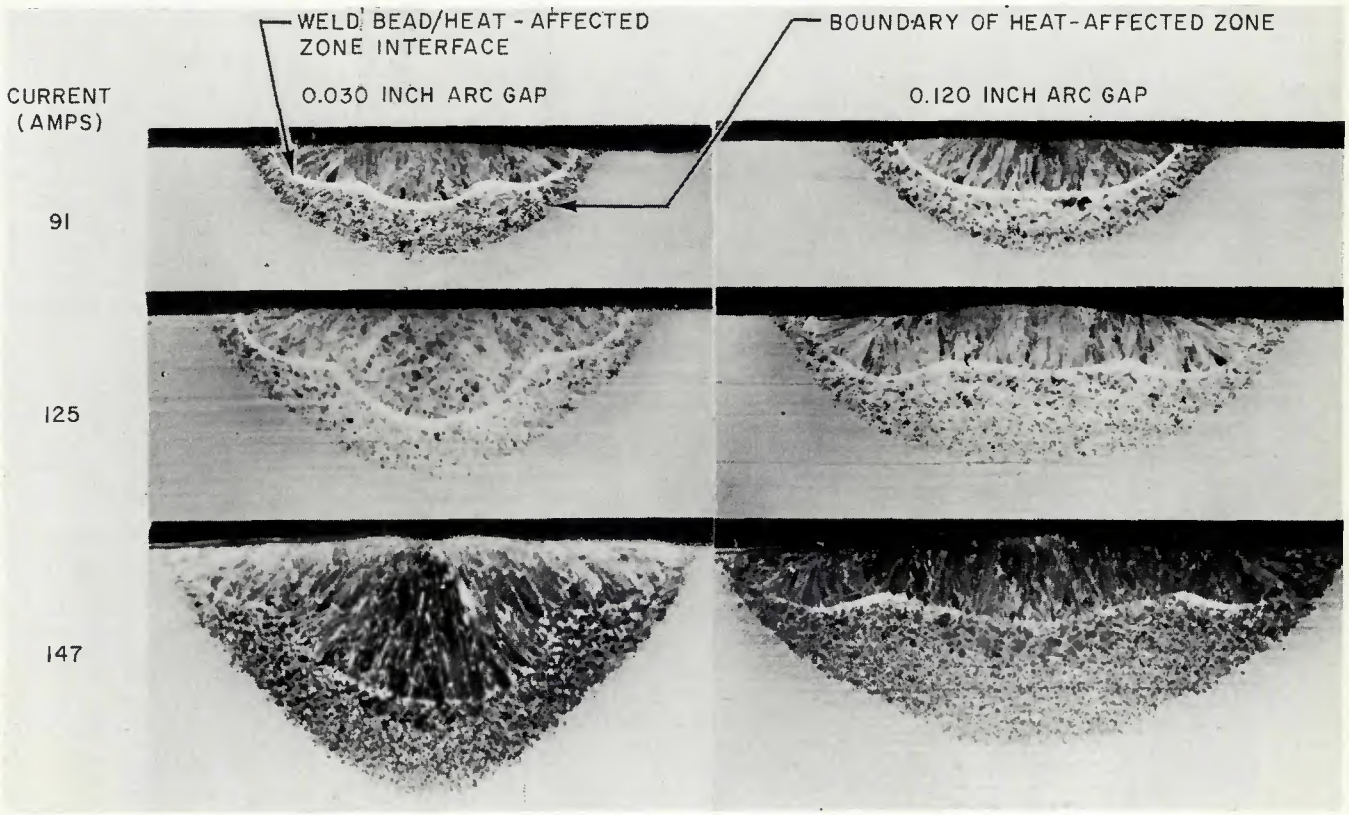

Fig. 1—Cross sections of stationary arc welds on 2 × 2 × ¼ in. (50.8 × 50.8 × 6.4 mm) alloy 600 plate. 10 second arc duration. ×10 (reduced 21% on reproduction)

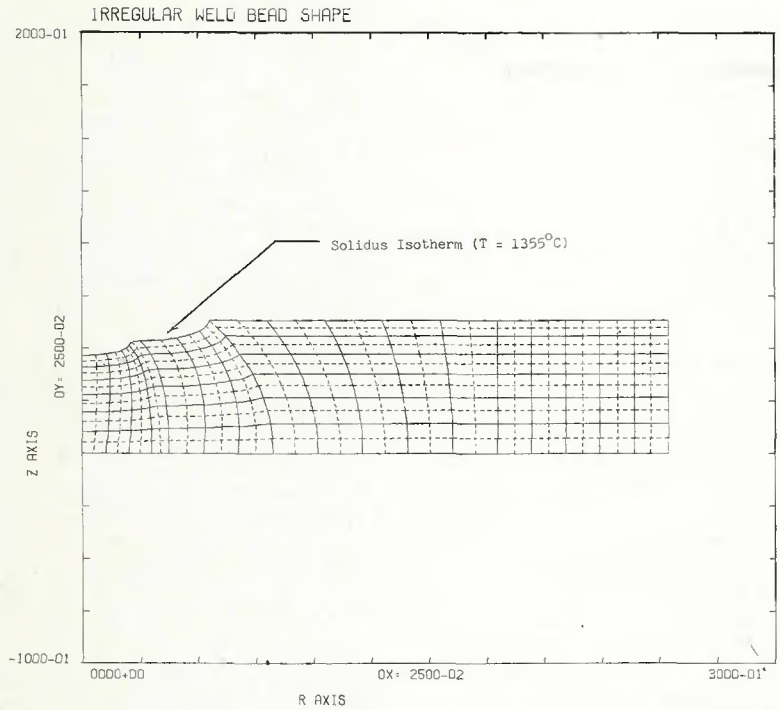

Fig. 2—Finite element mesh employed for heat conduction calculations

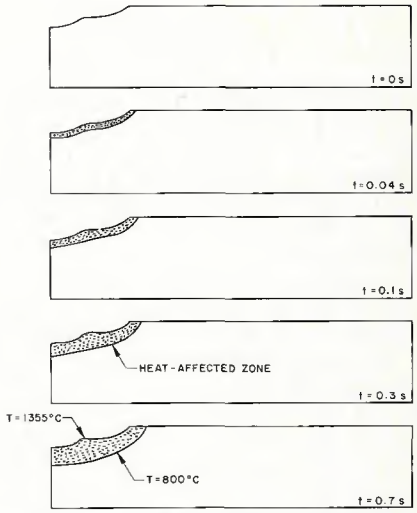

Fig. 3—Growth of heat-affected zone with time t. From top to bottom, t = 0, 0.04, 0.1, 0.3 and 0.7 second, respectively

the "humped" configuration of the boundary between the weld bead and the heat-affected zone shown in Fig. 1. It is also believed that this irregularly shaped boundary denotes the farthest extent of the melting isotherm during welding. For alloy 600, the melting temperature is between 1355 and 1400°C (2471 and 2552°F). Most recently Savage *et al.*[5] have reported similar observations and have associated this "humped" weld bead with the effect of arc pressure.

Regardless of the cause of such a peculiar bead shape, it is intuitively not apparent why the boundary between the heat-affected zone and the base metal is not irregularly shaped as well, since it is located a short distance from the irregularly shaped weld metal/heat-affected zone interface (Fig. 1) and would, therefore, be expected to be affected by the humped weld bead configuration. However, photomicrographs of stationary arc welds in alloy 600 plates show a smooth, ellipsoidal contour outlining the heat-affected zone. This is clearly illustrated in Fig. 1. Informal discussions of these observations at recent technical meetings have produced no definitive explanations as to why the heat-affected zone boundary is ellipsoidal.

To help explain this anomaly and thus provide a basis for understanding the observations, thermal calculations designed to simulate conduction heat flow conditions in the base metal and heat-affected zones of an alloy 600 weldment were performed. The results of these calculations are consistent with the observations of an ellipsoidal boundary demarcating the outer region of the heat-affected zone and provide a rational explanation for such observations. This brief note summarizes these results.

Calculational Model

A finite element analysis computer code was employed to calculate the heat flow in the heat-affected zone and base metal region of an alloy 600 weld plate. Heat input boundary conditions representing the existence of an irregularly shaped molten weld pool boundary resulting from a stationary heat source were used. The heat conduction equation for the axisymmetric temperature distribution T (r,z,t) is given by:

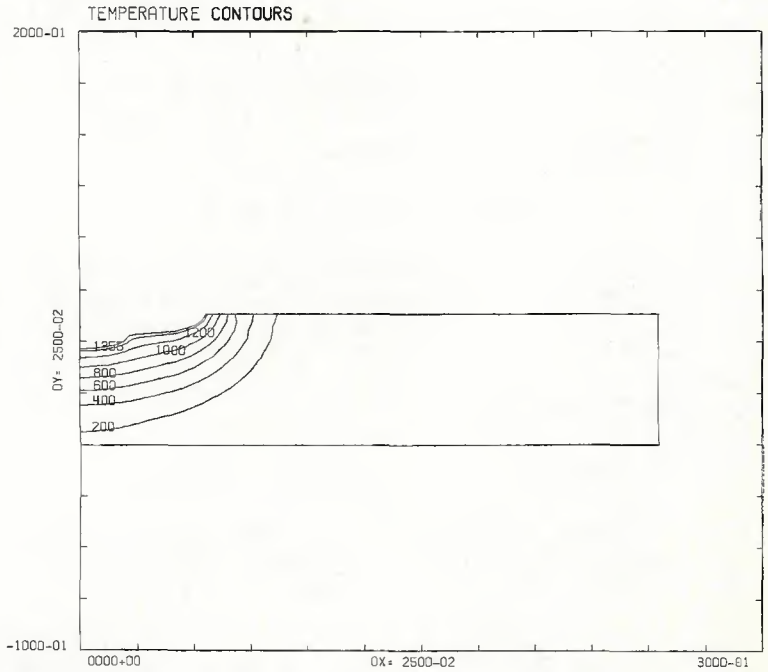

Fig. 4—Calculated isotherms (°C) in weldment at t = 0.7 second

S. S. GLICKSTEIN and E. FRIEDMAN are with the Bettis Atomic Power Laboratory operated for the U. S. Department of Energy by Westinghouse Electric Corp. in West Mifflin, Pennsylvania.

$$\frac{1}{r}\frac{\delta}{\delta r}\left(rk\frac{\delta T}{\delta r}\right) + \frac{\delta}{\delta z}\left(k\frac{\delta T}{\delta z}\right) = \rho c\frac{\delta T}{\delta t}$$

where T = temperature in weld plate; r = radial distance from center of heat source; z = axial distance from undersurface of weld plate; t = time from initial application of heat source; k = conductivity; ρ = density; c = specific heat.

Temperature dependent material properties of alloy 600 previously presented in the literature[2] were used.

Figure 2 illustrates the finite element mesh employed for these calculations. The solidus isotherm representing the maximum extent of the weld pool was maintained at 1355°C (2471°F). Heat losses at the surface of the weldment were accounted for by combined radiation q_r and natural convection q_c losses, which are given by:

$$q_r = \epsilon\,\sigma\,(T\text{-}T_o)^4$$
$$q_c = h\,(T\text{-}T_o)^{1.25}$$

where: ϵ = emissivity; σ = Stefan Boltzman constant; h = convection coefficient; T = surface temperature; T_o = ambient temperature.

The irregularly shaped boundary of the weld pool is incorporated directly into the finite element model as shown in Fig. 2. The weld pool boundary is maintained at a fixed temperature (1355°C) (2471°F), and heat is allowed to flow into the weldment continuously. The temperature of the alloy 600 plate increases with time, and the isotherm defining the boundary of the heat-affected zone is gradually enlarged. The heat-affected zone is denoted by the 800°C (1472°F) isotherm.

The growth of the heat-affected zone with weld time is shown in Fig. 3. At time t = 0.7 second (s), the area of the heat-affected zone is comparable to that of the experimentally observed heat-affected region (I = 91A, Fig. 1). Representative isotherms throughout the weldment at this time are shown in Fig. 4.

Results and Conclusions

The results of these calculations clearly illustrate that the mechanism of conduction heat transfer is sufficient to rapidly transform the irregular, humped shape of the melting isotherm to the ellipsoidal shape of the isotherm representing the boundary of the heat-affected zone, even though the two isotherms are in close proximity to each other. Figure 3 graphically demonstrates that within only 0.1 s of the start of welding, the shape of the 800°C (1472°F) isotherm representative of the heat-affected zone boundary is nearly regular. As time is increased to 0.3 s, the heat-affected zone grows into a regular, though not yet ellipsoidal, shape. The ellipsoidal shape is obtained at 0.7 s, at which time the locations and shapes of the 1355 and 800°C (2471 and 1472°F) isotherms are very similar to the weld metal and heat-affected zone boundaries, respectively.

These results illustrate the effectiveness of computer modeling for providing a rational explanation of why the shapes of weld metal and heat-affected zone interfaces can differ so distinctly. The employment of such modeling techniques continues to expand.[6,7] However, reliance on such analytical treatments to successfully predict the effects of welding processes can develop only through continued application and comparison of results with experimental data.

References

1. Glickstein, S. S., Friedman, E., and Yeniscavich, W. 1975. Investigation of alloy 600 welding parameters. *Welding Journal.* 54(4): pp. 113-s to 122-s.
2. Friedman, E., and Glickstein S. S. 1976. An investigation of the thermal response of stationary gas tungsten arc welds. *Welding Journal.* 55(12): pp. 408-s to 420-s
3. Ishizaki, K. 1969. Behavior of molten pool on vertical steel plate heated by stationary TIG arc. IIW Doc. SG 212-160-68, March.
4. Woods, R. A., and Milner, D. R. 1971. Motion in the weld pool in arc welding. *Welding Journal.* 50(4): pp. 163-s to 173-s.
5. Savage, W. F., Nippes, E. F., and Agusa, K. 1979. Effect of arc force on defect formation in GTA welding. *Welding Journal.* 59(7): pp. 212-s to 224-s.
6. Jones, Jr., R. F., Armen, H., and Fong, J. T., Eds. 1977. *Numerical Modeling of Manufacturing Processes.* ASME Publication PVP-PB-02S.
7. Engineering Foundation. 1980. Abstracts of "Modeling of Casting and Welding Processes" Conference. Rindge, New Hampshire, August 3-8.